Journal of Zhejiang University SCIENCE A
ISSN 1673-565X (Print); ISSN 1862-1775 (Online)
www.zju.edu.cn/jzus; www.springerlink.com
E-mail: jzus@zju.edu.cn

Bond strength improvement of GFRP rebars with different rib geometries*

HAO Qing-duo†1, WANG Yan-lei[1], ZHANG Zhi-chun[1], OU Jin-ping†‡1,2

([1]*School of Civil Engineering, Harbin Institute of Technology, Harbin 150090, China*)

([2]*School of Civil & Hydraulic Engineering, Dalian University of Technology, Dalian 116024, China*)

†E-mail: haoqingduo@163.com; oujinping@hit.edu.cn

Received Jan. 25, 2007; revision accepted May 11, 2007

Abstract: Based on the Canadian Standards Association (CSA) criteria, 105 pullout specimens were tested to investigate the effect of different rib geometries on bond strength of glass fiber reinforced polymer (GFRP) rebars embedded in concrete. Two kinds of conventional reinforcing rebars were also studied for comparison. Each rebar was embedded in a 150 mm concrete cube, with the embedded length being four times the rebar diameter. The experimental parameters were the rebar type, rebar component, rebar diameter, rebar surface texture, rib height, rib spacing and rib width. Theoretical analysis was also carried out to explain the experimental phenomena and results. The experimental and theoretical results indicated that the bond strength of GFRP rebars was about 13%~35% lower than that of steel rebars. The bond strength and bond-slip behavior of the specially machined rebars varied with the rebar type, rebar diameter, rebar surface texture, rib height, rib spacing and rib width. Using the results, design recommendations were made concerning optimum rib geometries of GFRP ribbed rebars with superior bond-slip characteristics, which concluded that the optimal rib spacing of ribbed rebars is the same as the rebar diameter, and that the optimal rib height is 6% of the rebar diameter.

Key words: GFRP rebars, Concrete, Pullout test, Bond strength, Rib geometries, Optimal surface configuration
doi:10.1631/jzus.2007.A1356 **Document code:** A **CLC number:** TU599; TB332; TU377.9

INTRODUCTION

Many concrete structures such as marine structures, bridge and parking garages subjected to aggressive environment, combined with moisture, temperature, and chlorides, reduce the alkalinity of concrete and result in corrosion of steel bars (ACI 440 Committee, 2001). The corrosion process causes concrete deterioration. Therefore, how to enhance the durability of the RC structure is a problem that needed to be solved immediately in civil engineering (Hao *et al*., 2007a). Professionals have always faced the challenge of corrosion decay in different ways. Methods such as galvanization, the use of stainless steel rebars, cathodic protection systems, epoxy coatings, concrete additives, polyester polymer concrete, etc., have been used (Okelo and Yuan, 2005; Ehsani *et al*., 1997; San-José *et al*., 2005). Although they are effective in some situations, these methods may still be unable to completely eliminate the problems of steel corrosion.

The use of fiber reinforced polymer (FRP) reinforcing bars to replace steel reinforcing bars has emerged as one of many techniques to enhance the corrosion resistance of reinforced concrete structures. FRP rebars produced in recent years appear to be a suitable candidate and have great potential to fill such a need (Tighiouart *et al*., 1998). These rebars have several important advantages over conventional reinforcing steel, namely, high tensile strength, light weight, non-corrosiveness, anti-fatigue, non-magnetic, electrical insulation, small creep deformation and specific gravity, and so on (Hao *et al*., 2006).

However, there are a number of issues related to the behavior of FRP rebars which need to be addressed. One of the issues is the brittle failure of FRP rebars in tension. Though the tensile strength of FRP

‡ Corresponding author

* Project (No. 200431882021) supported by the Western Communication Construction and Science & Technological Project, China

rebar is larger than that of steel rebar, the typical stress-strain relationship of FRP rebars is fairly linear at all stress levels up to the point of failure, without exhibiting any yielding characteristics like that observed for steel rebar (Benmokrane *et al*., 2000). But the most important factor limiting the field application of FRP rebars to civil engineering is the lack of information and design guidelines on their properties of bonding to concrete (Cosenza *et al*., 1997). The bond property between FRP rebars and concrete is affected not only by concrete strength, concrete cover, casting depth, embedded length, rebar diameter and ambient temperature (Katz and Berman, 2000), but also by the rebar's component and the outer surface, such as the rib spacing, rib height and rib face angle (Malvar *et al*., 2003). Therefore, the key problem for the research on the bond property between FRP rebars and concrete is to determine the optimal surface configuration first.

It is worth noting that a number of bond tests have already been performed by several experts on FRP rebars (Benmokrane *et al*., 1996; Achillides and Pilakoutas, 2004; Tighiouart *et al*., 1999; San-José and Manso, 2006; Hao *et al*., 2007b). However, these tests were localized to examine the effect of different surface configurations on the bond behavior, rather than research to determine the optimal surface configuration for FRP rebars specially. Based on 105 pullout specimens, this paper used the pullout test to study the bond behavior of glass fiber reinforced polymer (GFRP) ribbed rebars to concrete, and determine the optimal surface configuration finally.

Furthermore, the data presented here can be used to calculate the development length of GFRP ribbed rebars and establish the bond-slip constitutive relationship between GFRP ribbed rebars and concrete. This study's findings should be of interest to design engineers, manufactures, and those involved in development of code provisions.

EXPERIMENTAL PROGRAM

GFRP rebar

The GFRP rebars used in this research program were divided into 6 series in a total of 24 different rib geometries. Two kinds of steel ribbed rebars in nominal diameters of 10 and 12 mm were also tested for comparison. For each rebar, the rib spacing (RS) is the center-to-center spacing of the rebar ribs. Rib height (RH) is the height of the rib above the surface of the rebar, and is measured as the difference between the bar radius at a rib and the radius at midpoint between that rib and the next one. Rib angle (RA) is the angle that the rebar rib forms with the longitudinal axis of the ribbed rebar.

These rebars were manufactured using the pultrusion process and were made of thermosetting resin and Type E glass fibers. During manufacturing, different methods of surface treatment were adopted to enhance the bond between GFRP rebar and concrete. The surface configurations of GFRP rebars and steel rebars are shown in Fig.1. For series A and B rebars, one small fiber strand was wound in helical pattern on the rebar surface to make ribs before heat-curing, and was stripped off the rebar at last. For series C and F rebars, the longitudinal fibers were wrapped in a helical pattern with a small strand fiber which was

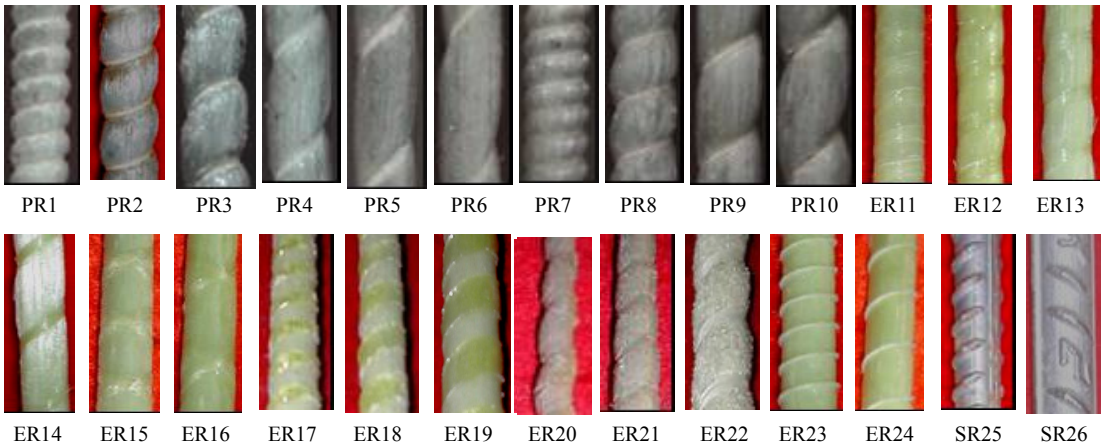

Fig.1 Surface configurations of GFRP rebars and steel rebars

tight to induce indentations on the surface and to improve its bond behavior, or were wound with fiber strands to make deformations on the surface before the heat-curing. For series D rebars, the ribs on the rebar surface were made by one 6 mm wide plastic strip. The strip was wrapped helically on the rebar surface, and was stripped off the rebar at last. Series E rebars named Aslan 100 were made by Hughes Brothers Inc., USA. This kind of rebar was sand coated with helical lengthwise ribs like series A and B rebars. Series G rebars were ordinary steel rebars. The surface treatment and deformation geometry of GFRP rebars and steel rebars are described in Table 1.

Table 1 Surface treatment and deformation geometry of GFRP rebars and steel rebars

Firm	Rebar notation	Diameter (mm)	Surface texture of GFRP rebar							
			Rope winding	Sand coating	Fiber strand winding		Surface deformation or rib			
					Single	Double	Deformation	Rib	RS (mm)	RH (mm)
A	PR1	10	−	−	+	−	−	+	5	0.6
	PR2*	10	−	−	+	−	−	+	10	0.6
	PR21*	10	−	−	+	−	−	+	10	0.4
	PR22*	10	−	−	+	−	−	+	10	0.5
	PR23*	10	−	−	+	−	−	+	10	0.7
	PR24*	10	−	−	+	−	−	+	10	0.8
	PR25*	10	−	−	+	−	−	+	10	0.9
	PR3	10	−	−	+	−	−	+	15	0.6
	PR4	10	−	−	+	−	−	+	20	0.6
	PR5	10	−	−	+	−	−	+	25	0.6
	PR6	10	−	−	+	−	−	+	30	0.6
B	PR7	12	−	−	+	−	−	+	6	0.6
	PR8#	12	−	−	+	−	−	+	12	0.6
	PR81#	12	−	−	+	−	−	+	12	0.36
	PR82#	12	−	−	+	−	−	+	12	0.48
	PR83#	12	−	−	+	−	−	+	12	0.72
	PR84#	12	−	−	+	−	−	+	12	0.84
	PR9	12	−	−	+	−	−	+	18	0.6
	PR10	12	−	−	+	−	−	+	24	0.6
C	ER11	10	−	−	+	−	+	−	10	0.32
	ER12	10	−	−	+	−	+	−	15	0.25
	ER13	10	−	−	+	−	+	−	20	0.20
	ER14	10	−	−	+	−	+	−	25	0.14
	ER15	10	−	−	−	+	+	−	20	0.21
	ER16	10	−	−	−	+	+	−	25	0.28
D	ER17	8	−	−	+	−	−	+	8	0.32
	ER18	8	−	−	+	−	−	+	12	0.44
	ER19	8	−	−	+	−	−	+	16	0.46
E	ER20	6.5	−	+	+	−	−	+	21	0.49
	ER21	9.5	−	+	+	−	−	+	17	0.81
	ER22	12.7	−	+	+	−	−	+	25	0.75
F	ER23	10	+	−	+	−	−	+	10	0.68
	ER24	10	+	−	+	−	−	+	15	0.79
G	SR25	10	−	−	−	−	−	+	7	1.00
	SR26	12	−	−	−	−	−	+	8	1.05

PR: GFRP rebar reinforced with polyester resin; ER: GFRP rebar reinforced with epoxy resin; SR: ordinary steel rebar; * and #: GFRP rebars with the same rib spacing; +: means to improve bond available; −: not available; RS: spacing of rib or deformation; RH: height of rib or deformation

Pullout specimen

For the experimental determination of the bond-slip relationship between rebar and concrete, pullout specimen with centric rebar placement can be used. This method is popular because it provides a simple means of comparing the relative bond behavior developed by different rebars. A sketch of the pullout specimen is shown in Fig.2. Each rebar was embedded in a 150 mm concrete cube, and the embedded length was four times ($4d$) the rebar diameter (CSA, 2002). All the rebars were 550 mm long. The length of the deformed GFRP rebars left on the loaded end was 380 mm, in order to satisfy the load requirements; on the free end the length left was 20 mm, so that we can measure the slip on the free end.

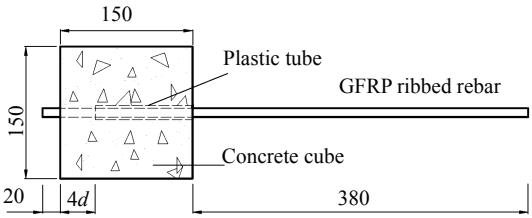

Fig.2 Sketch of pullout specimen (unit: mm)

Contact between the concrete and the rebar along the embedded length is broken using a soft plastic tube to equalize the stress from the loading plate on the loaded end side and minimize the stress concentration near the boundaries. Three nominally identical specimens were tested for each rebar to check the reliability of the test setup and the scatter of the test results. The concrete was cast vertically, and rodded 25 times with 16 mm diameter tamping rod. After molding, the specimens were cured by covering them with plastic sheet to prevent moisture loss for 28 d. During this period, the specimens were sprayed with water so as to maintain moisture on the surfaces all the time.

A four-part notation system was used to indicate the test variables of each pullout specimen. The first part of the notation indicates the rebar series: A, B, C, D, E, F or G; the second part of the notation indicates the nominal rebar diameter: 6.5, 8, 9.5, 10, 12 or 12.7 mm; the third part indicates the rib spacing: the value of the real center-to-center rib spacing; and the fourth part is the rib height in percent of the rebar diameter: ranging from 2% to 10%. The variables of all test specimens are identified in Table 2.

Testing equipment

The load frame used in this test was made according to (CSA, 2002), which is shown in Fig.3. The bond specimen was put into the frame, and the frame can be connected with the testing machine using a sleeving made specially. The steel plate had a hole through which the GFRP ribbed rebar can pass, with the hole diameter being 2 times the rebar diameter. A spherical seat was put between the channel steel plate and the lower plate, which ensures that the deformed GFRP rebar is subjected to the axial loads, not the torsional or flexural loads.

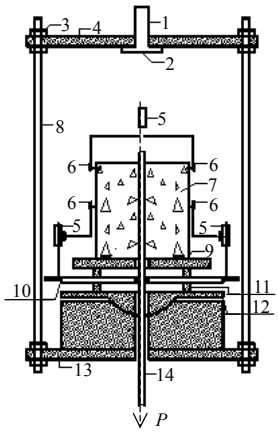

1: steel rebar; 2: cushion cap; 3: bolt; 4: upper plate; 5: LVDT; 6: LVDT rack; 7: bond specimen; 8: bolt rod; 9: steel plate; 10: gripper rack; 11: channel steel plate; 12: spherical seat; 13: lower plate; 14: GFRP ribbed rebar

(a)

(b)

Fig.3 Setup of pullout test. (a) Sketch; (b) Photo

The slips of the rebar relative to concrete at the loaded end and at the free end were measured with three linear variable differential transformers (LVDTs). On the loaded end, two LVDTs were

Table 2 Test results of pullout test specimens

Specimen notation	Test parameters				Test results			
	Rebar notation	RS (mm)	RH (mm)	f_c' (MPa)	P (kN)	τ (MPa)	s (mm)	Failure mode
A-10@5#0.06	R1	5	6%d	28.5	16.55	13.17	1.82	CS
A-10@10#0.06	R2	10	6%d	28.5	17.55	13.96	2.37	CS
A-10@15#0.06	R3	15	6%d	28.5	16.62	13.22	3.36	CS
A-10@20#0.06	R4	20	6%d	28.5	13.39	10.66	3.85	CS
A-10@25#0.06	R5	25	6%d	28.5	13.14	10.46	4.42	CS*
A-10@30#0.06	R6	30	6%d	28.5	13.37	10.64	4.68	CS*
A-10@10#0.04	R21	10	4%d	28.5	14.76	11.74	1.74	CS
A-10@10#0.05	R22	10	5%d	28.5	16.86	13.42	2.25	CS
A-10@10#0.07	R23	10	7%d	28.5	17.11	13.62	2.56	CS*
A-10@10#0.08	R24	10	8%d	28.5	12.90	10.26	1.86	CS*
A-10@10#0.09	R25	10	9%d	28.5	16.12	12.83	2.19	CS*
B-12@6#0.05	R7	6	5%d	28.5	16.70	9.23	1.34	CS
B-12@12#0.05	R8	12	5%d	28.5	21.00	11.61	2.49	CS
B-12@18#0.05	R9	18	5%d	28.5	19.60	10.83	4.18	CS
B-12@24#0.05	R10	24	5%d	28.5	17.00	9.39	4.40	CS
B-12@12#0.03	R81	12	3%d	28.5	14.60	8.07	3.39	CS
B-12@12#0.04	R82	12	4%d	28.5	19.60	10.83	3.08	CS
B-12@12#0.06	R83	12	6%d	28.5	23.50	12.99	2.74	CS
B-12@12#0.07	R84	12	7%d	28.5	18.20	10.06	2.63	CS*
C-10@10#0.03	R11	10	3.2%d	26.3	13.72	10.92	2.62	DS
C-10@15#0.03	R12	15	2.5%d	26.3	12.95	10.31	3.85	DS
C-10@20#0.02	R13	20	2%d	26.3	12.43	9.90	3.61	DS
C-10@25#0.01	R14	25	1.4%d	26.3	10.86	8.65	3.34	DS
C-10@20#0.02	R15	20	2.1%d	26.3	12.35	9.83	1.66	DS
C-10@25#0.03	R16	25	2.8%d	26.3	15.38	12.25	3.42	DS
D-8@8#0.03	R17	8	3.2%d	27.4	10.73	13.34	3.03	DS
D-8@12#0.06	R18	12	5.5%d	27.4	13.54	16.84	5.70	DS
D-8@16#0.06	R19	16	5.8%d	27.4	15.26	18.97	4.71	DS
E-6.5@21#0.05	R20	21	4.9%d	27.4	11.26	21.21	2.34	CS*
E-9.5@17#0.08	R21	17	8.1%d	27.4	21.80	18.44	0.60	CS*
E-12.7@15#0.08	R22	15	7.5%d	27.4	23.46	11.57	3.32	CS*
F-10@10#0.07	R23	10	6.8%d	26.3	9.61	7.65	2.48	DD
F-10@15#0.08	R24	15	7.9%d	26.3	8.80	7.01	4.16	DD
G-10@7#0.1	R25	7	10%d	27.4	26.70	21.25	1.08	CS
G-12@8#0.09	R26	8	10.5%d	27.4	37.45	20.70	1.24	CS

d: rebar diameter; f_c': the concrete compressive strength; τ is average bond strength; P is applied pullout load; s: the slip at the loaded end; CS: the shear of concrete between the ribs; CS*: the shear of concrete between the ribs, with the ribs being slightly damaged; DS: the shear of the deformation; DD: the desquamate of the deformation

clamped to the rebar using the gripper rack, which measured the relative displacement. They were diametrically opposed to compensate for any rotation. A third LVDT was located on the free end to measure the relative displacement between the concrete and the unloaded end of the rebar.

The testing machine for pullout tests must be capable of accurately applying the prescribed load. The load applied to the rebar must be at a rate not greater than 22 kN/min or at a no-load speed of the testing machine head that must not be greater than 1.27 mm/min. In this test, the testing machine was the INSTRON Series 5500R electronic universal material testing machine with a capacity of 100 kN. All the tests were carried out in displacement control mode at a speed of 0.5 mm/min so as to obtain the postpeak behavior. The load was measured with the electronic load cell of the machine. Output from the testing machine and the three LVDTs was recorded using an automatic data acquisition system. Loadings and readings were continued until: (1) pull-through or rupture of the GFRP ribbed rebar occurs; (2) the en-

closing concrete splits; or (3) slippage of at least 5 mm has occurred at the loaded end with the load nearly remaining the same.

EXPERIMENTAL RESULTS

Mode of failure

The type of failure observed for each test is given in Table 2. In most cases the specimens failed by the shear of concrete between the ribs of the rebar, which is called pullout failure. But the damage of the rib, the shear off of the deformation, or the desquamation of the deformation was also observed. Pullout failure occurred once the shear strength of bond between the rebar and the concrete was exceeded. The ultimate bond strength of the specimens was dictated by the shear strength of the concrete surrounding the rebar and the rib geometries of the rebar.

Average bond strength

Assuming uniform bond strength distribution along the embedded length in concrete, the average bond strength is defined as the shear force per unit surface area of the rebar. The average bond stress, τ, at any stage during loading is the applied pullout load on the bar, P, divided by the nominal surface area of the embedment length l_a of the bar. For a circular bar diameter d, this is given by the relationship:

$$\tau = P/(\pi d l_a), \tag{1}$$

where, τ is average bond strength in MPa; P is applied pullout load in N; d is diameter of the rebar in mm; and l_a is embedded length in mm.

Slip at the loaded end

Due to the low elastic modulus of GFRP ribbed rebars, this elongation is significant and has to be corrected. The slip at the loaded end was calculated, taking into account the adjustment for the elastic elongation of the rebar between the actual loaded end of the embedment length and the attachment point of the LVDTs, as given below:

$$s = s_m - \delta_e, \tag{2}$$

$$\delta_e = PL/(E_f A_f), \tag{3}$$

where, s is the slip at the loaded end in mm; s_m is the measured slip in mm; δ_e is the slip correction due to rebar elongation in mm; P is applied pullout load in N; L is the length between the top surface of bonded length and the average point of attachment of the LVDTs on the rebar in mm; E_f is the modulus of elasticity in MPa; and A_f is the nominal cross sectional area in mm^2.

Test results for all the bond specimens are given in Table 2.

ANALYSIS OF EXPERIMENTAL RESULTS

Effect of rebar type

The bond-slip curves of GFRP rebars and ordinary steel rebars are shown in Fig.4. Compared to steel rebars, GFRP rebars showed lower bond strength only about 65%~87% of the former, and the slip at the loaded end of GFRP ribbed rebar was larger, too. This difference in the bond can be attributed to the difference of the surface rib geometries of each type of rebar. For steel rebar, the bearing component is the major source of the bond. The rib of GFRP rebar does not possess the characteristics of steel rebars (i.e. high shear strength, high rigidity and rib geometries) that provide enough lateral confinement through rib bearing.

Effect of rebar component

The bond-slip curves of GFRP rebars with different component are shown in Fig.5. The component of series A rebar was type E glass fiber and polyester, and the volume content of the fiber was 72%. The component of series C rebars was type E glass fiber and epoxy resin, and the volume content of the fiber was 64%.

From Fig.5 it can be seen that these two types of rebars exhibited similar bond behavior. The bond strength at the same rib spacing of 10 mm was 11.74 MPa and 10.92 MPa, respectively. And the slip at the loaded end was 1.74 mm and 2.62 mm, respectively. Considering the effect of the difference in rib height, the effect of rebar component on bond behavior was neglectable. The reason for this phenomenon was that the physical and mechanical properties of ribs did not improve with the variation of the rebar component.

Effect of rebar diameter

The bond-slip curves of GFRP rebars are shown in Fig.6. It can be seen from Fig.6 that the bond strength decreased, but that the slip at the loaded end increased when the diameter of the rebar increased. The smaller bond strength of big diameters can be explained by the bleeding of the water in concrete. The bigger the diameter of the rebar, the higher the quantity of bleeding water trapped beneath the rebar, creating a greater void. This void reduced the contact surface between the rebar and the concrete and hence the bond strength decreased.

Effect of rebar surface texture

The bond-slip curves of rebars with different surface textures are shown in Fig.7. From Fig.7 it can be seen that the bond strength of rebars in series D and F was lower than the other series, and that the slip at the loaded end was bigger than that of the other series. Therefore, the surface texture of series D and F rebars was not suggested.

For the rebars of series C, the bond strength of rebars wrapped with double helix fiber strand was still large when the rib spacing was 2.5 times the rebar large when the rib spacing was 2.5 times the rebar diameter. It can be concluded that the surface texture made of double helix fiber strand can improve the bond behavior of GFRP rebar effectively.

The GFRP rebars of series A and E had similar rib geometries, but the rebars of series E were sand coated. The bond strength of series E rebars was bigger than that of series A rebars, and the slip at the loaded end of the former was smaller than that of the latter. Therefore, the treatment of sand-sprayed on the rebar surface was an effective way to improve the bond behavior between GFRP rebar and concrete.

Effect of rebar rib spacing

In the A series, the bond strength, the slip at the loaded end and the bond-slip curves of rebars with different rib spacing are shown in Figs.8a, 8b and 9a.

It can be found that as the rib spacing increased from 1 to 3 times the rebar diameter with the relative

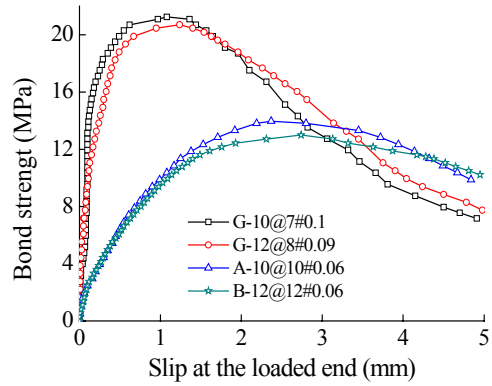

Fig.4 Bond-slip curves of different kinds of rebars

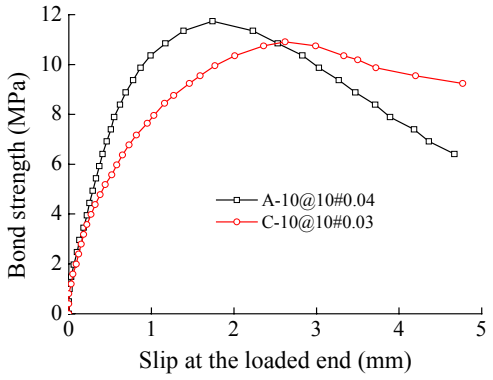

Fig.5 Bond-slip curves of GFRP rebars with different components

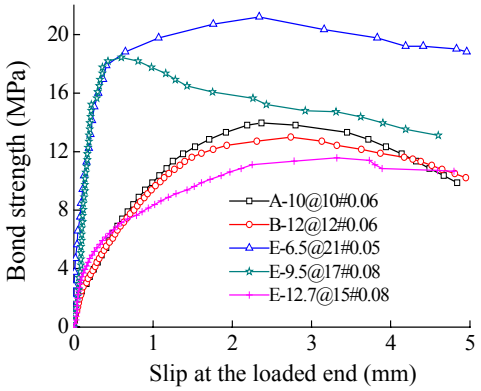

Fig.6 Bond-slip curves of GFRP rebars with different diameters

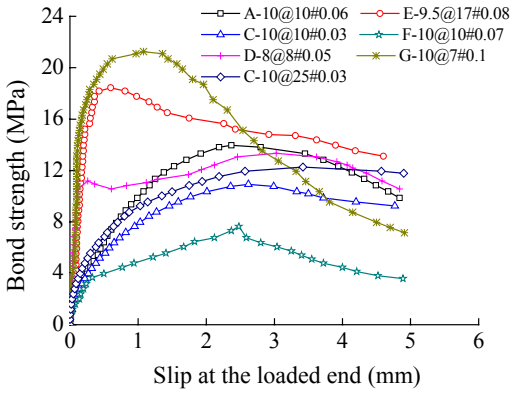

Fig.7 Bond-slip curves of rebars with different surface textures

rib area decreasing from 0.06 to 0.02, the peak bond strength and the slip corresponding to a given load (bond stiffness) decreased, and the loaded end slip at failure increased by two times. The slip at failure of rebars with rib spacing of 50%*d* was a little smaller than that of rebars with rib spacing being the same as the rebar diameter, but the peak bond strength of the former was less than that of the latter, while the former slope of the curve after the peak point was larger than the latter. Therefore, the GFRP ribbed rebar with rib spacing being the same as the rebar diameter gave the highest peak bond strength and the best bond-slip behavior as compared with rebars with rib spacing ranging from 50% to three times the rebar diameter.

Effect of rebar rib height

In the B series, the bond strength, the slip at the loaded end and the bond-slip curves of rebars with different rib height are shown in Figs.10a, 10b and 9b. It can be found that as the rib height increased from3%*d* to 6%*d*, the initial bond stiffness of the curve increased, and the peak bond strength of the ribbed rebar improved approximately 60%. But the improving trend was stopped when the rib height was increased to 7%*d*. Both the peak bond strength and the initial bond stiffness decreased obviously. And the slope of the curve after the peak point was larger than that of the rebar with rib height of 6%*d*, too. Therefore, the GFRP ribbed rebar with a rib height of 6%*d* developed the highest peak bond strength and the lowest slip for a given load.

Effect of rebar rib width

In the D series, the bond-slip curves of rebars with different rib width are shown in Fig.11. The clear rib spacing of these rebars was 6 mm, and the change of rib spacing was due to the rib width. The rib width of the rebars was 2 mm, 6 mm and 10 mm, respectively. It can be found that as the rib width increased from 2 mm to 6 mm, the initial bond stiffness of the curve decreased, but the peak bond strength of the ribbed rebars improved approximately 42%. Other

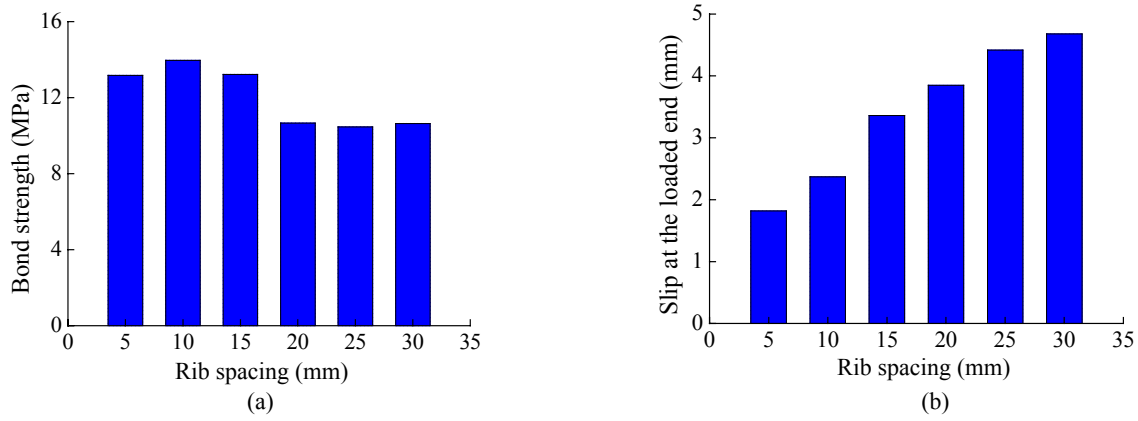

Fig.8 Bond strengths (a) and slips at the loaded end (b) of GFRP rebars with different rib spacing

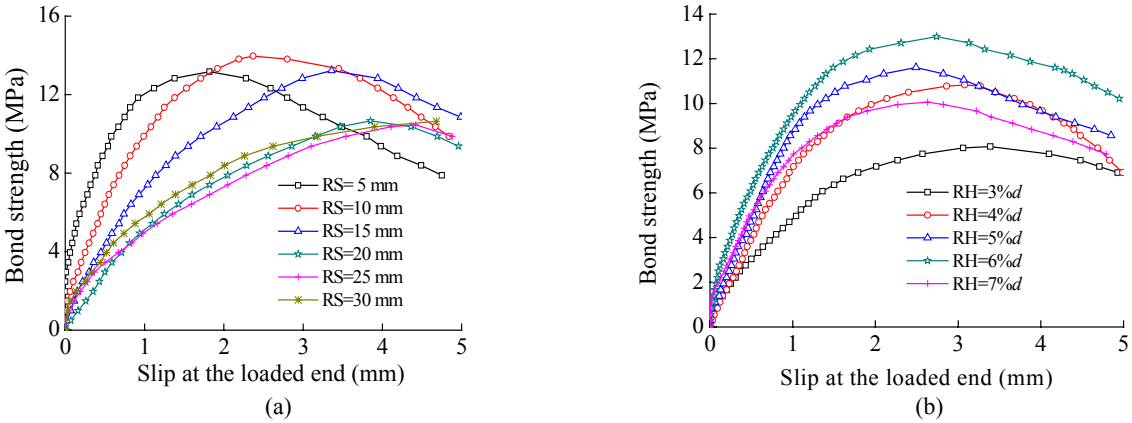

Fig.9 Bond-slip curves of GFRP rebars with different rib spacing (a) and rib height (b)

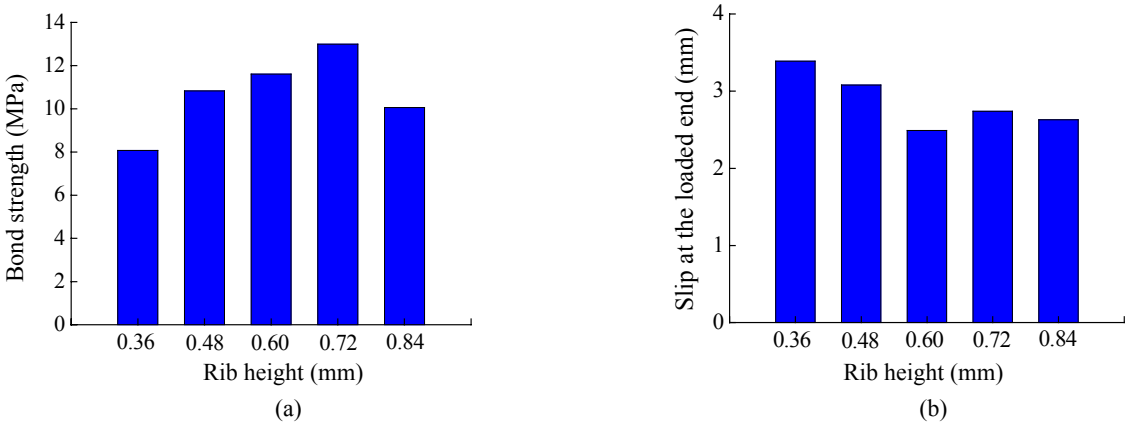

Fig.10 Bond strengths (a) and slips at the loaded end (b) of GFRP rebars with different rib height

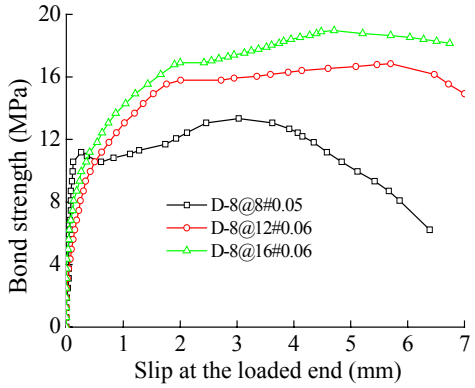

Fig.11 Bond-slip curves of GFRP rebars with different rib width

disadvantage was that the slip at the loaded end of the rebars was too large. Therefore, it is difficult to evaluate the bond behavior of rebars with different rib width, and further research is needed to determine the optimum rib width for GFRP ribbed rebars.

CONCLUSION

Results of the research program on GFRP ribbed rebars of 24 different rebars indicated similar trends. On the basis of the analysis and comparison of the test results of 105 pullout specimens, the following observations and conclusions can be made:

(1) The bond strength of the GFRP ribbed rebar depended primarily on mechanical interaction between the ribs of the rebar and the surrounding concrete. Therefore, the bond strength and bond-slip relationship of GFRP ribbed rebars varied with the rib geometries.

(2) The bond failure failed in the pull-through mode for most of the specimens. Concrete between the ribs at the loaded end was crushed; no signs of splitting cracks appeared on the cube. But, the damage of the rib, the shear off of the deformation, or desquamation of the deformation was also observed.

(3) The bond strength of GFRP ribbed rebar was lower than that of ordinary steel rebar, only about 65%~87% of the latter, and the slip at the loaded end of GFRP ribbed rebar was larger, too.

(4) The bond strength of GFRP ribbed rebar varied with the diameter and the surface texture of the rebar, but not the rebar component. The bond strength decreased with the increase of the rebar diameter, and improved highly when the surface was sand-coated or wrapped with double helix fiber strand.

(5) When the rib height of the test rebar was kept constant, the ribbed rebar with rib spacing being the same as that of the rebar diameter was superior to rebars with rib spacing ranging from 0.5 to 3 times the rebar diameter.

(6) When the rib spacing of the test rebar was kept constant, the ribbed rebar with rib height 6%d was superior to those with rib heights ranging from 3%d to 9%d.

(7) The effect of rib width on bond behavior of GFRP ribbed rebars was also of significance, and further research was needed to determine the optimum rib width.

(8) When different combinations of rib geometries were investigated, the non-sand coated ribbed rebar with rib spacing being the same as the rebar diameter, and rib height of 6%d developed the largest peak bond strength, stiffest bond-slip curve (greatest

bond strength for a given slip), least loaded end slip at failure, and the smallest slope of the curve after the peak point.

References

Achillides, Z., Pilakoutas, K., 2004. Bond behavior of fiber reinforced polymer bars under direct pullout conditions. *Journal of Composites for Construction*, **8**(2):173-181. [doi:10.1061/(ASCE)1090-0268(2004)8:2(173)]

ACI 440 Committee, 2001. Guide for the Design and Con-Struction of Concrete Reinforced with FRP Bars. American Concrete Institute, Detroit, Michigan, USA.

Benmokrane, B., Tighiouart, B., Chaallal, O., 1996. Bond strength and load distribution of composite GFRP reinforcing bars in concrete. *ACI Materials Journal*, **3**:246-253.

Benmokrane, B., Zhang, B.R., Chennouf, A., 2000. Tensile properties and pullout behavior of AFRP and CFRP rods for grouted anchor applications. *Construction and Building Materials*, **14**(3):157-170. [doi:10.1016/S0950-0618(00)00017-9]

Cosenza, E., Manfredi, G., Realfonzo, R., 1997. Behavior and modeling of bond of FRP rods to concrete. *Journal of Composites for Construction*, **1**(2):40-51. [doi:10.1061/(ASCE)1090-0268(1997)1:2(40)]

CSA (Canadian Standard Association), 2002. CSA S806 02 Design and Construction of Building Components with Fibre Reinforced Polymers. Canadian Standards Association International, Toronto, Canada.

Ehsani, M.R., Saadatmanesh, H., Tao, S., 1997. Bond behavior of deformed GFRP rebars. *Journal of Composites Materials*, **14**:1413-1430.

Hao, Q.D., Wang, B., Ou, J.P., 2006. Fiber reinforced polymer rebar's application to civil engineering. *Concrete*, **9**:38-40 (in Chinese).

Hao, Q.D., Wang, B., Ou, J.P., 2007a. Bond behavior between FRP rebar and concrete. *Architecture Technology*, **1**:15-17 (in Chinese).

Hao, Q.D., Zhang, Z.C., Wang, Y.L., Ou, J.P., 2007b. Comparison experimental study on bond behavior of deformed GFRP rebars with different outer surface. *FRP/CM*, **2**:37-39 (in Chinese).

Katz, A., Berman, N., 2000. Modeling the effect of high temperature on the bond of GFRP reinforcing bars to concrete. *Cement & Concrete Composites*, **22**(6):433-443. [doi:10.1016/S0958-9465(00)00043-3]

Malvar, L.J., Cox, J.V., Bergeron Cochran, K., 2003. Bond between carbon fiber reinforced polymer bars and concrete I: Experimental study. *Journal of Composites for Construction*, **7**(2):154-163. [doi:10.1061/(ASCE)1090-0268(2003)7:2(154)]

Okelo, R., Yuan, R.L., 2005. Bond strength of fiber reinforced polymer rebars in normal strength concrete. *Journal of Composites for Construction*, **9**(3):203-213. [doi:10.1061/(ASCE)1090-0268(2005)9:3(203)]

San-José, T.J., Vega, I., Ferreira, A., 2005. Reinforced polymer concrete: Physical properties of the matrix and static/dynamic bond behavior. *Cement and Concrete Composites*, **27**(9-10):934-944. [doi:10.1016/j.cemconcomp.2005.06.004]

San-José, T.J., Manso, J.M., 2006. Fiber-reinforced polymer bars embedded in a resin concrete: Study of both materials and their bond behavior. *Polymer Composites*, **27**(3):315-322. [doi:10.1002/pc.20188]

Tighiouart, B., Benmokrane, B., Gao, D., 1998. Investigation of bond in concrete member with fiber reinforced polymer FRP bars. *Construction and Building Materials*, **12**(8):453-162. [doi:10.1016/S0950-0618(98)00027-0]

Tighiouart, B., Benmokrane, B., Mukhopadhyaya, P., 1999. Bond strength of glass FRP rebar splices in beams under static loading. *Construction and Building Materials*, **13**(7):383-392. [doi:10.1016/S0950-0618(99)00037-9]